ELSEVIER

Thin Solid Films 423 (2003) 77–87

thin solid films

www.elsevier.com/locate/tsf

Characterization of highly hydrophobic coatings deposited onto pre-oxidized silicon from water dispersible organosilanes

A. Marcia Almanza-Workman[a,*], Srini Raghavan[a], Slobodan Petrovic[b], Bishnu Gogoi[b], Pierre Deymier[a], David J. Monk[b], Ray Roop[b]

[a]*Department of Materials Science and Engineering, University of Arizona, Tucson, AZ 85721, USA*
[b]*Motorola Inc., Sensor Products Division, Tempe, AZ 85284, USA*

Received 14 August 2002; received in revised form 14 August 2002; accepted 10 October 2002

Abstract

The formation and quality of highly hydrophobic coatings deposited from water dispersible organosilanes onto pre-oxidized single crystal silicon were studied using atomic force microscopy, ellipsometry, dynamic contact angle measurements and electrochemical impedance spectroscopy (EIS). Highly hydrophobic films of a commercially available water dispersible silane and two different cationic alkoxysilanes were prepared by dip coating. It was found using atomic force microscopy that, in general, the structure of these highly hydrophobic films is a continuous film with some particulates attributed to bulk polymerization of the precursor molecule in water. Film defects were quantified using EIS by the value of charge transfer resistance at the hydrofluoric acid/silicon interface. Potential applications of this type of coatings include reduction/elimination of stiction in micro-electromechanical systems, contact printing in materials microfabrication, inhibition of corrosion and oxidation, prevention of water wetting, lubrication and protein adsorption.

Keywords: Water dispersible organosilanes; Hydrophobic coatings; Stiction; Coating defects; Electrochemical impedance spectroscopy

1. Introduction

Highly hydrophobic coatings are being actively considered in silicon based micro-electromechanical systems to reduce adhesion that may be encountered during wet processing. Deposition of self-assembled monolayer (SAM) coatings is one of the most successful approaches to chemical modification of silicon surfaces in order to reduce adhesion in microstructures. This approach involves making the surfaces of pre-oxidized silicon and polysilicon hydrophobic, through the formation of SAM films [1–3]. By making the surface hydrophobic, the capillary attraction that collapses the microstructure when the surfaces are hydrophilic is greatly reduced. As a result, microstructures come out of the final water rinse extremely dry without being broken or adhered to the substrate. Extensive studies of SAMs of alkylchlorosilanes, alkylsiloxanes and alkylaminosilanes deposited from organic media onto silicon oxide surfaces have been reported [4].

High quality SAMs of alkyltrichlorosilane derivatives are not easy to form, mainly because of the need to carefully control the amount of water in the liquid medium used for deposition [5–7]. While incomplete monolayers are formed in the absence of water, excess water results in polymerization in the solution and polysiloxane deposition on the surface [8]. As a result, the solvents used for SAM coating with $RSiCl_3$ precursors must be highly anhydrous. For example, for octadecyltrichlorosilane (OTS) coatings, an alkane is used with 30 vol.% of a cosolvent such as carbon tetrachloride (CCl_4) or chloroform ($CHCl_3$) [9]. The role of CCl_4 is believed to help in dehydrating the structures prior to film formation, solvate OTS head group in the solvent mixture and rinse away excess OTS molecules, which may be physisorbed to the surface.

*Corresponding author. Tel.: +1-520-3222983; fax: +1-520-3222993.
E-mail address: almanzaa@u.arizona.edu (A.M. Almanza-Workman).

0040-6090/03/$ - see front matter © 2002 Elsevier Science B.V. All rights reserved.
PII: S0040-6090(02)00997-5

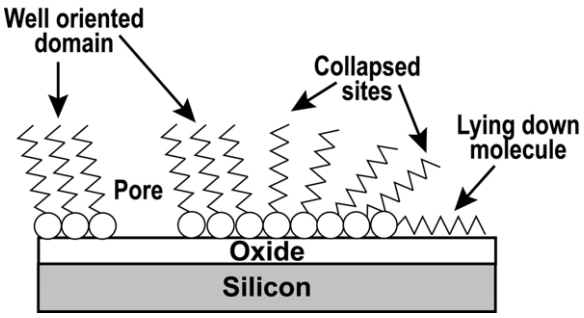

Fig. 1. Schematic representation of collapsed sites on the organosilane/silicon electrode.

The structure of alkylchlorosilanes SAMs on pre-oxidized silicon has been studied extensively [5,7,10–16]. Atomic force microscopy (AFM) studies [17–21] have shown the formation of both a dense organized assembly with vertically aligned hydrocarbon chains and domains with disordered molecules that have not self-assembled. The relative proportions of the different phases depend on water concentration, solution age, temperature [9,22,23], silane concentration, dispersion pH [24], exposure or reaction time and substrate pre-treatment [5]. The presence of large particulates that are up to several microns in diameter has been observed on OTS coatings prepared at 50% relative humidity and 20 °C [25].

Structural defects [26–28] that have been identified to exist on alkyl mercaptans and *n*-alkanethiols SAMs deposited on gold (Fig. 1) are: (i) *pinholes or pores* where no molecules are adsorbed onto the surface, (ii) '*lying-down*' molecules near these pinholes that in fact cover the defects and (iii) *collapsed sites* where differently tilted molecules at the boundaries of differently oriented domains give rise to a thin layer. These defects have been characterized through their impact on electron-transfer reactions, which can be studied using electrochemical impedance spectroscopy (EIS) in aqueous chloride solutions. The largest electron-transfer rate constants were exhibited at sites with pores, somewhat smaller rate constants were found at the 'collapsed' sites, and the smallest values were obtained for well-oriented monolayers. Defect free coatings have the advantage of exhibiting very large energy barriers to carrier tunneling that makes them exceptional insulators for nanoscale devices [29].

In the case of coatings formed on oxidized silicon, hydrofluoric acid solutions can be effectively used to probe liquid penetration into the coatings. Hydrofluoric acid solutions upon penetration through the coating attack the oxide layer and thereby promote charge-transfer reactions at the Si/HF solution interface in the absence of dissolved oxygen. The corresponding charge-transfer reactions are [30,31]:

Anodic reaction: $Si_{(s)} + 6F^-_{(aq)} + h^+ \leftrightarrow SiF^{2-}_{6(aq)} + 4e^-$

$$E^0_{ox} = 1.2 \text{ V (SHE)}$$

Cathodic reaction: $Si_{(s)} + H^+ + e^- \leftrightarrow SiH$

$$E^0_{red} = -0.1 \text{ V (SHE)}$$

In this paper, we present the results of a study that explored different characterization methods to determine the quality of highly hydrophobic coatings deposited from aqueous media onto pre-oxidized single crystal silicon. Previous investigations have shown that this type of coatings yield contact angles greater than 100° when deposited onto pre-oxidized silicon as well as polysilicon [32–34].

2. Experimental

2.1. Materials

2.1.1. Chemicals

Two different organosilane systems were used in this study. The first chemical system consisted of a commercially available, proprietary, water dispersible octadecylsilane based compound (Siliclad®). This compound, obtained from Gelest, Inc., is reported to contain the reactive silane at a concentration of 20% in a mixture of tertiary alcohols and diacetone alcohol.

The second chemical system consisted of cationic alkoxysilanes [35] with two functional groups: one that allowed physical adsorption and the other that promoted chemisorption onto silicon oxide at an optimized pH value. The cationic silanes chosen for detailed investigation (purchased from Gelest, Inc.) were *N*,*N*-Dimethyl-*N*-octadecyl-3-aminopropyltrimethoxysilyl chloride (DMOAP) and *N*,*N*-didecyl-*N*-methyl-3-aminopropyltrimethoxysilyl chloride (DIDAP). The presence of quaternary ammonium group also allows the silane to aggregate and disperse in the aqueous phase.

Semiconductor-grade 50:1 hydrofluoric acid (50 parts of water and 1 part of 49% HF solution) was obtained from Arch Chemicals, Inc.

2.1.2. Substrate

Two types of single crystal silicon (1 0 0) wafers were used; antimony doped n-type (0.02 Ω cm) cut into pieces of 1×1 cm^2 for EIS experiments and boron doped p-type (7–17 Ω cm) for ellipsometry, atomic force microscopy and contact angle measurements.

The silicon samples were cleaned prior to coating deposition in 4:1 H_2SO_4 (98%):H_2O_2 (30%) solution for 15 min at ~90 °C to remove organic contaminants, thoroughly rinsed in deionized (DI) water, then etched in 50:1 HF to remove the oxide film. In order to immobilize the organic silane monolayers on the substrate, the presence of Si–OH groups on the substrate surface is necessary to form a covalent bond between the monolayer and the substrate surface. Therefore, an

oxidation treatment with 30% H_2O_2 at 30 °C for 15 min was performed before deposition of a monolayer. This treatment yields hydrophilic surfaces with water contact angles of 0–20° and 18–20 Å thick oxide layers.

2.2. Coating preparation

The organosilanes were diluted in DI water (resistivity of 18 MΩ cm) before use and adjusted with acetic acid to a pH value of 4. Dispersions containing 0.5, 1 and 3% reactive silane component of Siliclad® and 0.1% reactive silane of DMOAP and DIDAP were prepared. The dispersions containing cationic alkoxysilanes were heated to 35 °C and kept at this temperature during the coating process.

The coatings were deposited onto the substrates by immersing the samples into the silane dispersions at 400 μm/s and withdrawing at 40 μm/s (for Siliclad® coatings) or 400 μm/s (for DIDAP and DMOAP films). Delay times of 10 min between immersion and withdraw steps were necessary only for Siliclad® coatings. These conditions (immersion speed, withdrawal speed and delay time) were obtained by using a 2^k factorial design of experiments to optimize hydrophobicity and coating thickness. The film-covered substrates were cleaned by rinsing with DI water and finally blow-dried with nitrogen. Curing of Siliclad® coatings was done in a convection oven for 10 min at 200 °C.

2.3. Methods

2.3.1. Spectroscopic ellipsometry

Ellipsometric film thickness measurements were carried out using a variable angle spectroscopic ellipsometer (VASE) from J.A. Woollam Co. The ellipsometric parameters ψ (amplitude ratio) and Δ (phase change) were measured at three different incidence angles (70, 75 and 80°) over the 2000–6000 Å range. The composite optical constants (n and k) of the silicon substrate with the thin oxide film were calculated and taken as baseline for thickness calculation of the organosilane films. Since optical constants of SAMs were not available for the wavelength range used, it was assumed that the organic film had the same optical properties as silicon dioxide. Ellipsometric measurements were taken immediately before and after coating each sample.

2.3.2. Contact angle measurements

Hydrophobicity of the coatings was determined by measuring the contact angle of DI water immediately after film deposition using a dynamic contact angle analyzer (Cahn DCA-312).

2.3.3. Atomic force microscopy

AFM measurements were performed on a Dimension 3000 microscope system (Digital Instruments, Inc.) operated in a tapping mode. All measurements were performed in air using commercial silicon cantilevers with spring constants of 20–100 N/m and resonance frequency of 300–350 kHz. Data analysis was performed with the Digital Instruments NanoScope III version 5.12r2 software. The depth of pores and height of particulates on the coating were determined from cross-sectional profiles at several random locations for each AFM image.

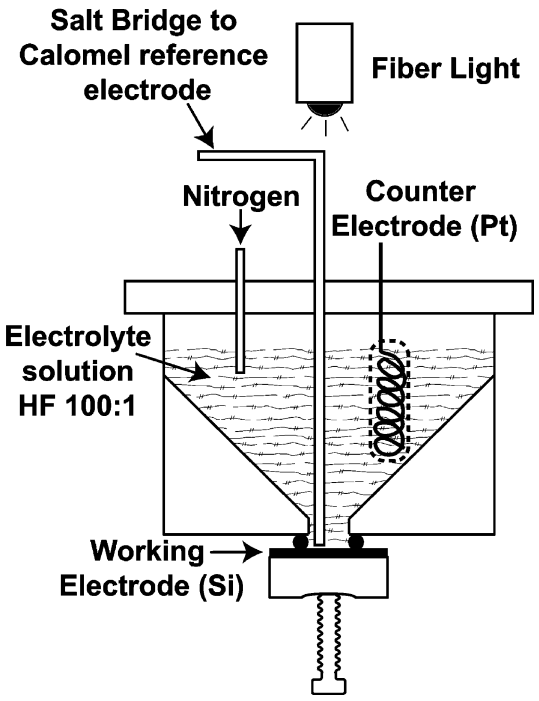

Fig. 2. A schematic sketch of the cell used for the electrochemical characterization of coated and uncoated silicon surfaces in HF solutions.

2.3.4. Electrochemical impedance spectroscopy

Electrochemical experiments were performed using a three-electrode cell made of Teflon with a polystyrene transparent cover (Fig. 2). The calomel reference electrode was always immersed in 4 M KCl and isolated from the cell by a salt bridge made of Teflon capillary tube filled with KCl (3 M) gelled in agar. The counter electrode was a platinum spiral immersed in a plastic tube to prevent hydrogen bubbles from disturbing the system. The working electrode was antimony doped single crystal silicon (0.02 Ω cm) with a sample area of 0.18 cm^2 as defined by a Viton® O-ring. The top of the cell was irradiated with an optical fiber lamp (30 W) at its maximum intensity. Solutions were purged with nitrogen gas for a minimum 1 h before each electrochemical experiment and kept under a nitrogen atmosphere during the course of the experiment. All experiments were conducted using high purity (ppb grade) 100:1 HF (100 volumes H_2O, 1 volume 49%

Table 1
DI water contact angles and film thicknesses determined by Ellipsometry

Coating[a]	Thickness (Å)		Contact angle (°)		
	Expected	Spectroscopic ellipsometer	Advancing	Receding	f_{CH_3}
0.5% Siliclad®	N/A	5.2±0.3	94.3±0.7	72.1±1.0	0.02
1% Siliclad®	N/A	8.9±0.4	96.4±2.7	74.3±1.4	0.05
3% Siliclad®	N/A	44.5±15.8	109.1±1.2	91.3±0.8	0.95
0.1% DMOAP	22.6[b]	20.7±8.5	99.1±1.6	59.8±1.8	0.36
0.1% DIDAP	12.6[b]	7.6±0.7	98.9±1.2	77.2±2.4	0.35
0.1% DMOAP/0.05% Siliclad®	–	20.9±4.5	101.2±1.1	67.0±0.4	0.50
0.1% DIDAP/0.5% Siliclad®	–	6.4±0.3	94.5±2.0	73.8±0.6	0.04
OTS (low humidity) [32]	28.1	–	110±2	97±2	1.0
OTS (50% RH) [16,22]	26.5	–	106±2	80±2	0.79

[a] The percentage indicated refers to the percent of reactive silane in the aqueous dispersion.
[b] From molecular modeling in vacuum using HYPERCHEM v3.0.
N/A: Not available due to proprietary information from Gelest.

HF) to avoid formation of oxide at the bottom of the pores in the coating. The oxide on the backside was removed by gently rubbing the surface with a small cotton tip soaked in HF solution, followed by Ni printing to obtain ohmic contact. For coated samples, the reverse side was sanded with alumina paper to remove the coating prior to Ni printing.

Electrochemical measurements were carried out using an EG&G frequency response detector model 1025 connected to a Potentiostant/Galvanostant (EG&G model 283). The impedance data were automatically acquired using M398 electrochemical impedance software (EG&G). EIS responses of uncoated and coated antimony single crystal silicon samples in 100:1 HF were obtained by applying single sine wave of 5 mV in the frequency range of 5×10^{-3} to 5×10^{6} Hz with 5 points per decade. The silicon-coated electrode was held at the open circuit potential for all EIS experiments to prevent any potential drift and possible voltage-dependent degradation of the coating. The impedance data was fitted to equivalent circuits using EQUIVCRT software (v 4.55) distributed by EG&G, which uses a nonlinear least square fit (NLLSF) technique. The quality of the fit was evaluated from the χ^2 values.

3. Results and discussion

Five coating systems were studied: Siliclad®, DMOAP, DIDAP, DMOAP/Siliclad® and DIDAP/Siliclad®. These last two were double coating systems, in which the first coating was deposited from either of the two cationic alkoxysilanes and the second one from Siliclad® dispersions containing 0.5% reactive silane. No delay time was imposed between immersion and withdrawal of the sample from the dispersion. This was done to improve the hydrophobicity and coverage of cationic alkoxysilanes coatings.

3.1. Layer thickness

The average film thickness values measured on five different regions on the coated samples are presented in Table 1. The calculations of film thickness from ellipsometry data are based on the assumption that all of the films have the same refractive index. The exact value of the refractive index cannot be derived with an acceptable degree of accuracy from Δ and ψ data for such thin layers. It has been reported [36] that refractive index depends on the size of alkylsilane and the structure of the layer, but its impact on the thickness values is roughly 10% or less.

The thickness of Siliclad® coatings was found to depend on reactive silane concentration. The coating thicknesses deposited from dispersions containing 0.5 and 1% reactive silanes were below the reported values for vertically oriented coatings of OTS (28.1 Å). The reason for this is the presence of a large number of 'lying-down' molecule defects. The coatings deposited from a dispersion containing 1% reactive silane showed higher thickness values as a result of increased silane coverage on the surface and/or decrease in defects. The thickness values of Siliclad® coatings deposited from dispersions containing 3% of reactive silane concentration were higher than the length of fully stretched alkylsilanes. This is more likely due to the deposition of particulates formed as a result of rapid oligomerization of the alkylsilanes in the aqueous phase prior to covalent bonding to the silicon surface [36] (Fig. 3). The lower concentration of organosilane retards oligomerization in the bulk but the hydrophobic character of the coatings decreases as described in the next section of this paper.

The thickness values of coatings prepared from dispersions containing cationic alkoxysilanes (DMOAP and DIDAP) correspond to molecular lengths and the thick-

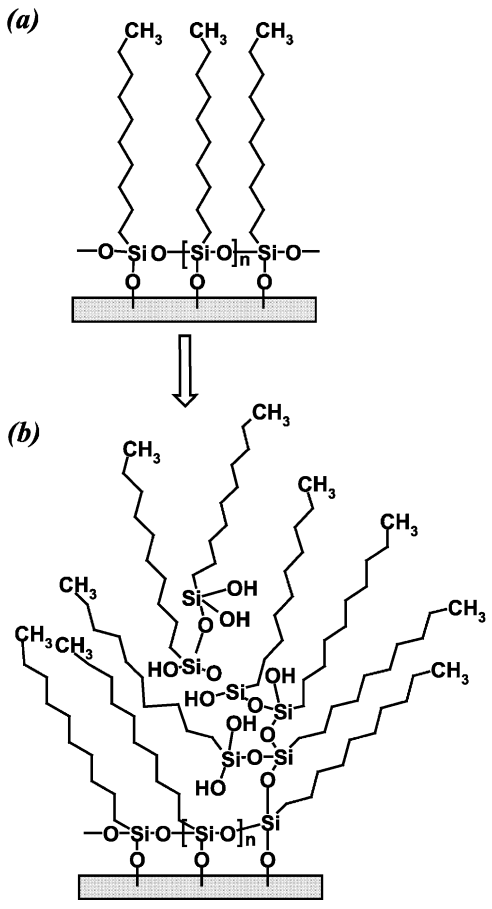

Fig. 3. (a) Self assembly versus (b) buildup organic film.

ness increases with alkyl chain length. The thickness of DMOAP coating is less than the length of the fully stretched octadecylsilane molecule, which could indicate a slightly disordered monolayer structure. Similar trends are observed for DIDAP coatings.

The thickness of DMOAP/Siliclad® and DIDAP/Siliclad® double coating systems did not change after the first coating, likely due to the fact that these coatings are predominantly composed of cationic alkoxysilanes.

3.2. Wettability

The dynamic DI water contact angles on the different organosilane coatings are listed in Table 1. The advancing contact angles on these coatings were between 94 and 109° and the receding contact angles varied from 60 to 90°. The hysteresis between advancing and receding contact angle was higher for DMOAP surfaces than for Siliclad® and DIDAP surfaces. This may be attributed to a difference in molecular scale roughness and porosity of the coatings.

The advancing and receding contact angles reported in literature for coatings deposited from alkyltrichlorosilanes onto pre-oxidized silicon with disordered monolayer structure are 103–105° and 91–92°, respectively [36]. These contact angles are independent of the chain length. Highly ordered coatings of OTS have shown advancing and receding contact angles of 110 and 98°, respectively. SAMs show higher contact angles because of the exposure of the highly hydrophobic alkyl groups to the aqueous phase. Disordered monolayers were obtained for our coatings in most cases except for 3% reactive silane of Siliclad®. The increase in hydrophobicity of double coating systems could be an indication of improvement in coverage, assembly and/or orientation.

As a first evaluation of the degree of disorder, an approach developed by Israelachvili–Gee [36,37] was used. In this method, the wettability of an alkyl-coated surface is determined using relative contributions to wettability by methyl or methylene according to the following equation:

$$(1+\cos\theta_{exp})^2 = f_{CH_2}(1+\cos\theta_{CH_2})^2 + f_{CH_3}(1+\cos\theta_{CH_3})^2$$

where θ_{exp} = experimental advancing contact angle; θ_{CH_2} = contact angle for pure surfaces of methylene groups (94°); θ_{CH_3} = contact angle for pure surfaces of methyl groups (110°); f = fraction of methyl or methylene groups.

Using this equation, the fraction of the surface that is composed of methyl groups (f_{CH_3}) was calculated from the contact angle data as shown in Table 1. For highly ordered coatings, the surface is composed primarily of methyl groups. Methylene groups start to be exposed as the degree of disorder increases. The high values of f_{CH_3} and thickness for coatings prepared from dispersions containing 3% reactive Siliclad® could indicate the deposition of highly oriented films. On the other hand, coatings deposited from dispersions containing 0.5 and 1% reactive silane showed low fraction of methyl groups and low thickness values as a result of low packing and predominantly 'lying-down' molecules that form a liquid expanded phase. DMOAP and DIDAP coatings showed methyl fractions of $\sim$0.35 and by recoating with Siliclad® the methyl fraction was improved to 0.5 for DMOAP coatings, but for DIDAP coatings a reverse effect was observed ($f_{CH_3} \sim 0.04$).

3.3. Uniformity and thickness

Fig. 4 shows a set of AFM images of coatings prepared from Siliclad® dispersions on pre-oxidized silicon as a function of reactive silane concentration. These images provide evidence that Siliclad® coatings prepared from dispersions containing 0.5% reactive silane (Fig. 4a) are composed of a continuous film with some particulate features which are 4–6 Å in height. Black spots in the image maybe identified as pores in the continuous film and their relative depth is roughly 5 Å. An increase in reactive silane concentration from

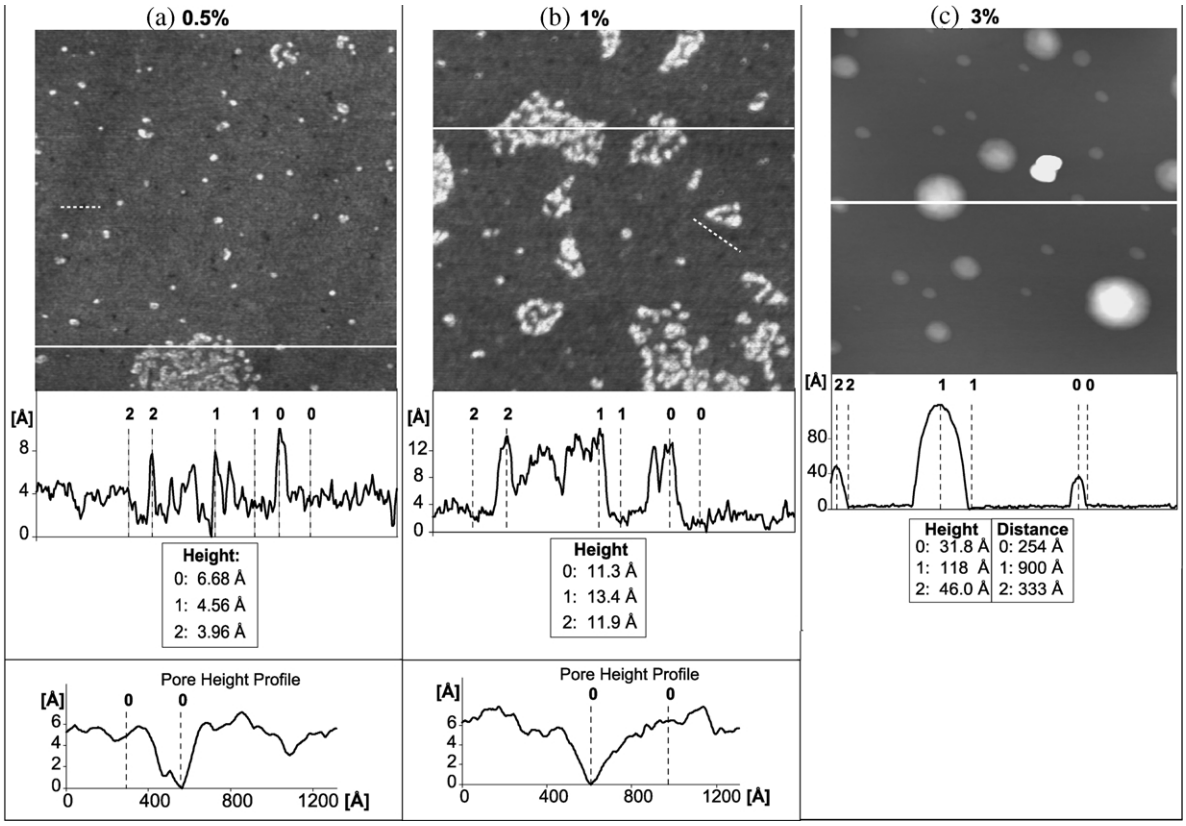

Fig. 4. AFM images, of a 1×1 μm^2 region, showing Siliclad® coatings on single crystal silicon substrates. (Height profiles in the lower part of the image were measured along the horizontal white lines. The pore height profiles were measured along the dotted lines.)

0.5 to 1% caused the particulates to grow laterally and vertically to a size of 11–13 Å in height and the relative pores depth to 6.5 Å (Fig. 4b). The film deposited from a 3% reactive silane dispersion (Fig. 4c) is characterized by large particles with vertical dimensions of 30–120 Å and lateral dimensions of hundreds of Å. These particulates are most likely formed as a result of silane crosslinking in the bulk. The advancing and receding contact angles for this coating are higher than for coatings prepared from lower silane concentration dispersions. The presence of particulates in the bulk of deposited films does not seem to be detrimental to the hydrophobic character of the films. The formation of these particulates has also been observed on OTS and DDMS coatings when deposited under humid conditions [25].

Fig. 5 shows an AFM image of a DMOAP film with the corresponding height profiles of particulates and pores. The particulates consist mainly of aggregates with uniform height of 40 Å and some with small features of 58 Å in height. These values correspond to bilayers and trilayers of DMOAP molecules. The pore depth was found to be 4.5 Å.

The number of particulates on top of the double coating system DMOAP/Siliclad® (Fig. 6) appears to be lower than that observed for DMOAP (Fig. 5) and Siliclad® (Fig. 4a) coatings. This could be as a result of additional rinsing steps that were used to remove excess silane from the surface. The height of particulates was 35–42 Å, which is similar to DMOAP particulates. The pore depth was found to be 7.0 Å.

The pore depths in DMOAP and DMOAP/Siliclad® coatings were smaller than their respective film thicknesses measured using spectroscopic ellipsometry (Table 1). This could be due to the tip not reaching the substrate at the bottom of the pores.

Imaging of DIDAP and DIDAP/Siliclad® coatings was extremely difficult. An experiment was conducted in which one half portion of a pre-oxidized silicon sample was rapidly etched in HF and the unetched area was then coated with DIDAP. AFM analysis showed a gradual change in surface roughness at the expected boundary but no evidence of characteristic features or particulates. It is possible that these films were free of pores and particles. Further work will be necessary to elucidate these findings.

3.4. Defects

EIS is a useful technique to characterize thin insulating films at electrode surfaces and can be particularly sensitive to the presence of pores or pinholes in films.

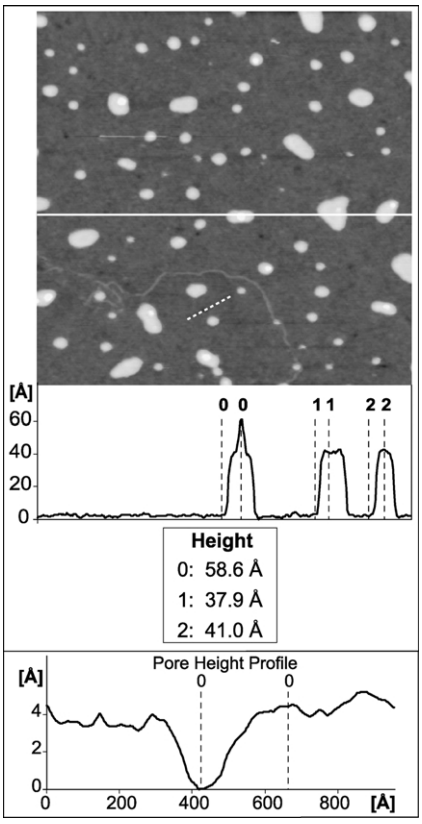

Fig. 5. AFM image (1×1 μm^2) of DMOAP coating. (Height profiles in the lower part of the image were measured along the horizontal white lines. Pore height profiles were measured along the dotted lines.)

In this work, the impedance of silicon/HF solution and silicon/coating/HF solution interfaces was analyzed using equivalent circuits. It was possible in this way to calculate interfacial resistance and capacitance that can be related to the quality of the films. The relative magnitude of these components provides an estimation of the protection provided by the coating against HF attack.

The equivalent circuits used to analyze the experimental data of uncoated and coated silicon samples are shown in Fig. 7. Because the experiments were carried out in HF solutions, no effects of oxide film were considered. In these circuits, R_{sample} is the sample bulk resistance and R_{sol} is the solution resistance. The sum of R_{sample} and R_{sol} will be referred to as R_0. The pore resistance (R_{pore}) that represents the resistance of pinhole type defect or chemical heterogeneity depends on the length of the pores and cross section. The capacitance C_{SC+DL} consists of the space-charge capacitance (C_{SC}) and the double layer capacitance (C_{DL}) in series; and has been commonly used for interpreting interfacial phenomena that occur at the silicon/HF solution interface [38,39]. The corresponding capacitance for a coated sample is C'_{SC+DL}. The interfacial charge-transfer resistance of uncoated and coated samples is R_t and R'_t, respectively. The values of R_t, C_{SC+DL} and R_{pore} for both coated and uncoated surfaces can be correlated to the area fraction of pore sites (θ) where silicon is in direct contact with HF [40]:

$$R'_t = \frac{R_t}{\theta}, \quad \theta C_{SC+DL} = C'_{SC+DL} \quad \text{and} \quad R_{pore} = \frac{R_{sol}}{\theta}$$

The coating and oxide capacitance is expressed in terms of a constant phase element (CPE). This is a 'power law-dependent' interfacial capacity, which accounts for the topography of imperfections and roughness of the substrate and coating. The impedance of CPE is given as:

$$Z_{CPE} = \frac{1}{Y_0(j\varpi)^n}$$

where Y_0 is the admittance and $n=1$ for an ideal capacitor [41].

The EIS spectra for both uncoated and coated silicon in HF solutions under illumination are shown in Figs. 8–11 in the form of Nyquist plots. The points in the figures represent the experimental data, while the solid lines represent the best fits obtained by the NLLSF

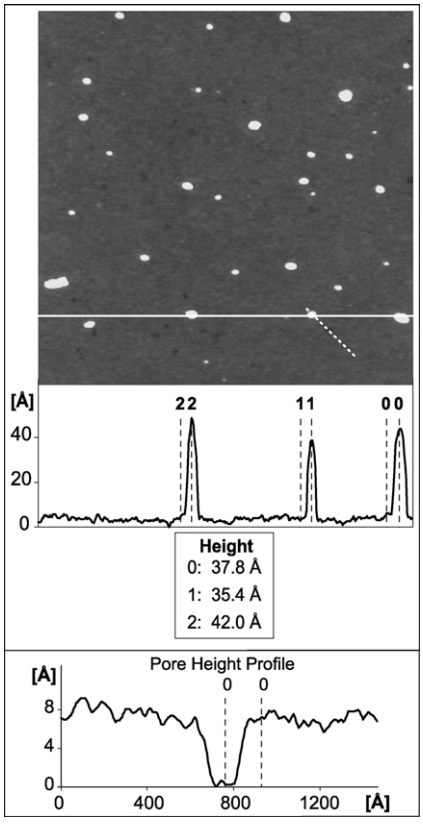

Fig. 6. AFM image (1×1 μm^2) of a DMOAP/Siliclad® coating. (Height profiles in the lower part of the image were measured along the horizontal white lines. Pore height profiles were measured along the dotted lines.)

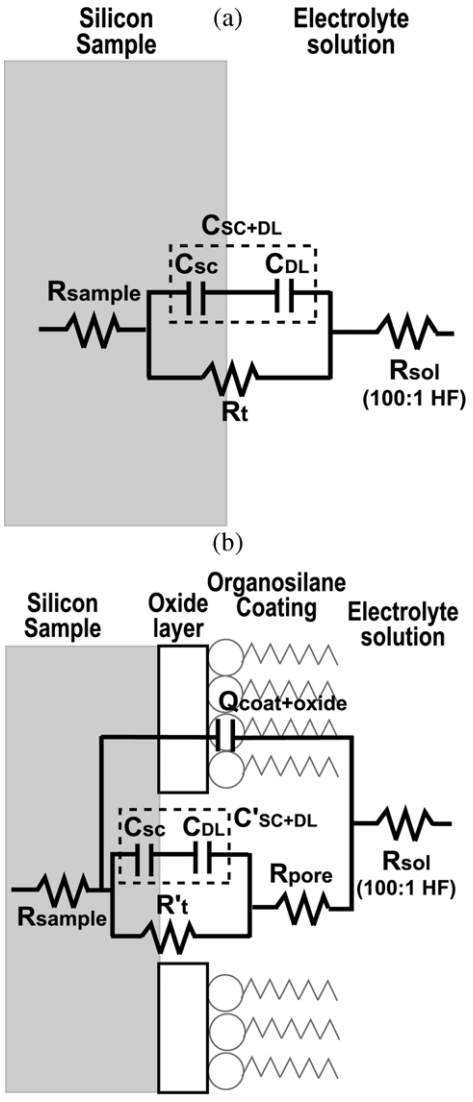

Fig. 7. Equivalent circuit used for the interpretation of impedance spectra obtained for (a) uncoated and (b) coated silicon/solution interface in 100:1 HF.

technique. In all cases, the spectra were characterized by one semicircle that represents a single time constant. Fig. 8 shows the Nyquist plots for Siliclad® coatings formed from solutions containing different levels of reactive silane. The diameter of the semicircles increased with silane concentration indicating that the coating was able to provide a much higher degree of resistance to charge transfer. The spectra for DMOAP and DIDAP coated surfaces are shown in Fig. 9. They appear quite similar to that for Siliclad® coated surfaces.

The parameters evaluated by fitting the experimental data to the equivalent circuits are summarized in Table 2. At least three newly prepared samples for each type of coating were analyzed to determine the reproducibility of EIS measurements.

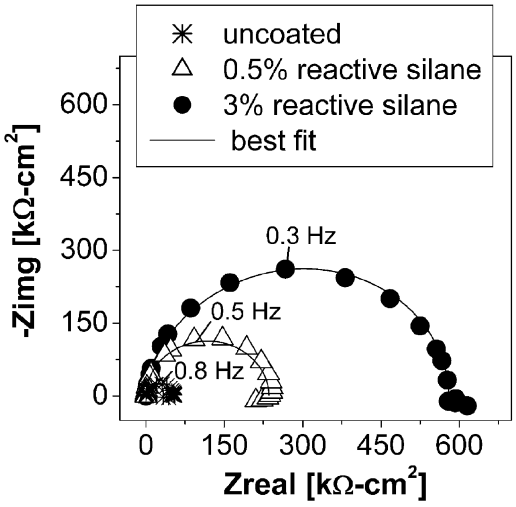

Fig. 8. Nyquist plots for Siliclad® coated silicon samples in 100:1 HF.

It is clear from the table that the R_t value for all coated surfaces is higher than that for uncoated surfaces. This implies that the electrochemical reactions proceed at lower rates when silane is deposited onto silicon. The very low value of charge transfer resistance for uncoated samples and the absence of Warburg component suggest that the electrochemical reaction at the silicon/HF solution interface is kinetically favorable and accelerated. The impedance in the low-frequency limit, R_t, significantly increased for all coated samples, especially for samples prepared from DMOAP and Siliclad® (3% reactive silane). The R_t value of Siliclad® coatings was dependent on the reactive silane concentration.

The values of R_0 (2–6 Ω cm^2) and R_{pore} (4–15 Ω cm^2) were found to be very small. This was expected because a highly doped sample and a high ionic strength

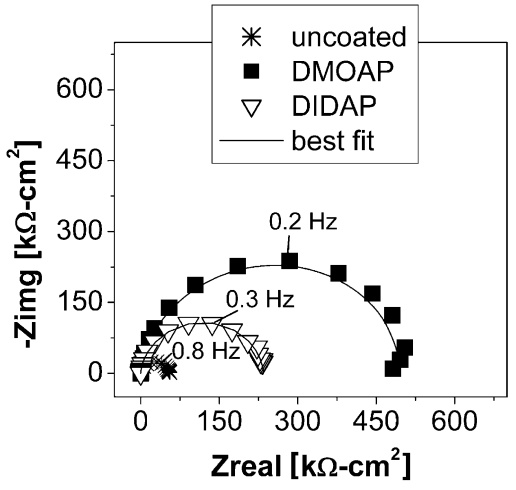

Fig. 9. Nyquist plots for DMOAP and DIDAP coated silicon samples in 100:1 HF.

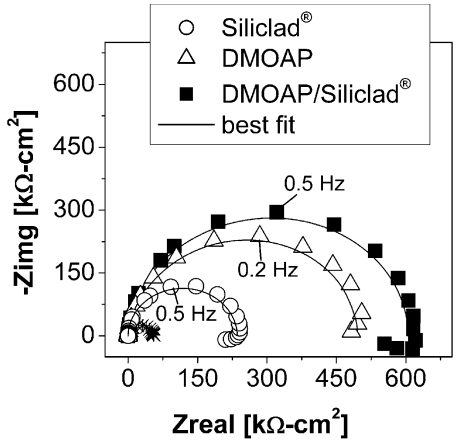

Fig. 10. Nyquist plots for single and double DMOAP/Siliclad® coatings on silicon samples in 100:1 HF.

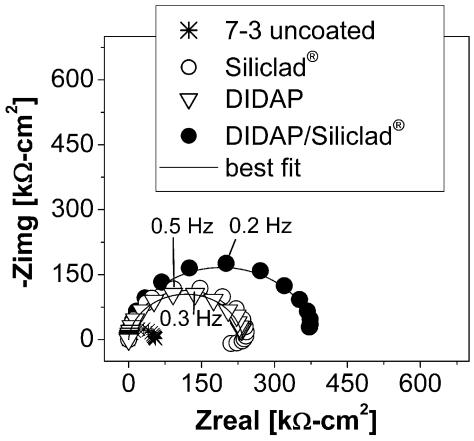

Fig. 11. Nyquist plots for single and double DIDAP/Siliclad® coatings on silicon samples in 100:1 HF.

solution (0.013 M) were used. The small variations in the value of R_0 could be caused by dilution inaccuracies.

Analysis of the coating capacitance can be used to examine the structure of the monolayer assemblies. For all coatings, the deviation of the CPE from ideal behavior (i.e. capacitor) was very small ($n>0.88$). Since the value of n does not depend on the length of the organosilane, Y_0 was assumed to be approximately equal to C_{coat} throughout [26].

According to Helmholtz model of the interface [42], the capacitance of the film is related to its thickness through the following equation:

$$Y_0 \approx C_{coat} = \frac{\varepsilon_{SAM}\varepsilon_0}{d_{SAM}}$$

where d_{SAM} is the thickness of the monolayer, ε_{SAM} is the total permittivity of the film and ε_0 is the permittivity of vacuum. The value of Y_0 for DIDAP (10 carbon atoms) was larger than for DMOAP (18 carbon atoms) as expected from their thickness values. Siliclad® (3% reactive silane) and DMOAP coatings had very similar Y_0 values because both organosilane molecules are composed of 18 carbon atoms. The lower Y_0 value for coatings prepared from dispersions containing 0.5% reactive silane of Siliclad® is a result of less organized films. This confirmed by thickness value obtained using ellipsometry.

Figs. 10 and 11 show the EIS spectra for double coatings systems. The R_t values increased from 450 and 200 kΩ cm² for DMOAP and Siliclad® single coating systems to 650 kΩ cm² for DMOAP/Siliclad® coatings and from 200 kΩ cm² for DIDAP to 350 kΩ cm² for DIDAP/Siliclad® coatings. This indicates that the defect levels in the film decreased by depositing a second silane layer. The charge-transfer resistance for DIDAP coatings was lower than for DMOAP and Siliclad® coatings, leading to conclusion that DIDAP coating is a poor barrier for electron transfer.

Table 2
Parameters obtained from the fitting of EIS data to equivalent circuits

	Sample						
	Uncoated	Siliclad® (0.5%)	Siliclad® (3%)	DMOAP	DIDAP	DMOAP/ Siliclad®	DIDAP/ Siliclad®
χ^2 ($\times10^{-3}$)	4.55±0.55	3.38±1.23	4.29±0.44	2.03±2.69	0.95±0.05	3.64±3.44	2.70±1.96
R_0 (Ω cm²)	6.52±3.76	2.29±1.50	3.35±0.37	5.11±1.61	3.06±2.10	6.66±5.89	1.47±1.07
$Y_{0\ COAT+OX}$ (μS/cm²)	–	0.47±0.21	0.83±0.09	0.90±0.31	1.96±0.41	0.66±0.38	2.10±0.48
$n_{COAT+OX}$	–	0.97±0.01	0.98±0.3	0.92±0.05	0.90±0.03	0.89±0.11	0.98±0.02
R_{pore} (Ω cm²)	–	5.18±1.47	11.31±3.55	16.57±12.09	3.73±0.94	6.92±2.29	2.68±1.86
C_{SC+DL} (μF/cm²)	2.67±0.43	–	–	–	–	–	–
C'_{SC+DL} (μF/cm²)	–	0.69±0.16	0.15±0.05	0.53±0.21	0.88±0.55	0.35±0.22	0.07±0.04
R_t (kΩ cm²)	59.39±5.45	–	–	–	–	–	–
R'_t (kΩ cm²)	–	220.63±37.00	553.55±26.13	451.90±49.59	236.71±5.75	668.65±62.68	369.48±27.45
θ_R	1.0	0.28±0.06	0.11±0.01	0.13±0.01	0.28±0.07	0.09±0.01	0.17±0.01
θ_C	1.0	0.26±0.06	0.07±0.02	0.19±0.08	0.32±0.21	0.13±0.09	0.03±0.02

The calculated values of area fraction of pore sites using R_t and C_{SC+DL} are tabulated in Table 2 as θ_R and θ_C. These values show reasonable agreement. The most important observation that can be made from the table is that the area fractions are between 0.1 and 0.3 indicating that the coatings are fairly compact.

The capacitance associated with the Helmholtz double layer was lower than for a typical metal or semiconductor electrode (>20 $\mu F/cm^2$) [39]. The same behavior has been observed by others [38] for n-type silicon exposed to 50:1 HF. From the equivalent circuit analysis, the value of the double layer capacitance was found to decrease for coated samples and was the lowest for coatings prepared from Siliclad® dispersions containing 3% reactive silane and from the double coating system DIDAP/Siliclad®. This effect is due to a decrease in the effective surface area of silicon as a result of surface coverage. It has been reported previously [38,43] that the surface coverage as a result of adsorption of organic molecules can reduce the double layer capacitance for semiconductor and metal electrodes from tens of microfarads to a few microfarads. The area fraction of pore sites (θ_C) calculated from the double layer capacitance is in agreement with the values obtained from charge-transfer resistance.

4. Conclusions

This study has shown that highly hydrophobic coatings can be reproducibly formed on pre-oxidized single crystal silicon wafers from a chemical system consisting of a commercially available water dispersible silane (Siliclad®) and/or cationic alkoxysilanes. Ellipsometric analysis indicates that thickness of these coatings is roughly a (statistical) monolayer. Wettability data show that the hydrophobicity and methyl (CH_3) fraction of the coatings exposed to solutions can be improved by increasing Siliclad® concentration in the dispersions and by the deposition of a double coating such as DMOAP/Siliclad®. AFM images show that the coatings deposited from dispersions containing low concentration of Siliclad® are thinner than the length of fully stretched alkyl chains in an octadecyl group. An increase in Siliclad® concentration increases the coating thickness, deposition and/or formation of particulates on the coating, as well as the contact angle. The DMOAP coatings consist of monolayers with small particulates and pores. EIS provides an effective method to determine the quality of the coatings by studying electron-transfer reactions between a coated silicon surface and HF solutions. The low pore fraction values determined by fitting the impedance data to equivalent circuits indicate that the coatings are reasonably compact.

Acknowledgments

Sensor Products Division from Motorola and National Science Foundation funded this work through the GOALI program under Grant No. 9905957. The authors would like to thank Andy Hooper and Xiang-dong Wang from Motorola for their technical assistance and AFM imaging. Special thanks go to Richard Workman and Bert Vermeire for AFM and EIS interpretation.

References

[1] R. Maboudian, W.R. Ashurst, C. Carraro, Sensors Actuators 82 (2000) 219.
[2] U. Srinivasan, M.R. Houston, R.T. Howe, R. Maboudian, J. Microelectromech. Syst. 7 (1998) 252.
[3] M.R. Houston, R. Maboudian, R.T. Howe, Solid State Sensor and Actuator Workshop, Hilton Head, SC, June 2–6 (1996) 42.
[4] A. Ulman, Chem. Rev. 96 (1996) 1533.
[5] J.D. Legrange, J.L. Markham, C.R. Kurkjian, Langmuir 9 (1993) 1749.
[6] C.P. Tripp, M.L. Hair, Langmuir 8 (1992) 1120.
[7] D.L. Angst, G.W. Simmons, Langmuir 7 (1991) 2236.
[8] S. Brandriss, S. Margel, Langmuir 9 (1993) 1232.
[9] A.N. Parikh, D.L. Allara, I.B. Azouz, F. Rondelez, J. Phys. Chem. 98 (1994) 7577.
[10] K. Kojio, A. Takahara, T. Kajiyama, Colloids Surf. A 169 (2000) 295.
[11] T. Vallant, J. Kattner, H. Brunner, U. Mayer, H. Hoffmann, Langmuir 15 (1999) 5339.
[12] H. Hoffmann, U. Mayer, A. Krischanitz, Langmuir 11 (1995) 1304.
[13] D.L. Allara, A.N. Parikh, F. Rondelez, Langmuir 11 (1995) 2357.
[14] H.O. Finklea, L.R. Robinson, A. Blackburn, B. Richter, D. Allara, T. Bright, Langmuir 2 (1986) 239.
[15] J. Sagiv, J. Am. Chem. Soc. 102 (1980) 92.
[16] S. Semal, M. Voue, M.J. De Ruijter, J. Dehuit, J. De Coninck, J. Phys. Chem. B 103 (1999) 4854.
[17] T. Vallant, H. Brunner, U. Mayer, H. Hoffmann, T. Leitner, R. Resch, G. Friedbacher, J. Phys. Chem. B 102 (1998) 7190.
[18] N.B. Sheller, S. Petrash, M.D. Foster, V.V. Tsukruk, Langmuir 14 (1998) 4535.
[19] C. Carraro, O.W. Yauw, M.M. Sung, R. Maboudian, J. Phys. Chem. B 102 (1998) 4441.
[20] S. Gauthier, J.P. Aime, T. Bouhacina, A.J. Attias, B. Desbat, Langmuir 12 (1996) 5126.
[21] S.R. Ge, A. Takahara, T. Kajiyama, Langmuir 11 (1995) 1341.
[22] R.R. Rye, Langmuir 13 (1997) 2588.
[23] J.B. Brzoska, N. Shahidzadeh, F. Rondelez, Nature 360 (1992) 719.
[24] E.J.A. Pope, J.D. Mackenzie, J. Non-cryst. Solids 87 (1986) 185.
[25] W.R. Ashurst, C. Yau, C. Carraro, R. Maboudian, M.T. Dugger, J. Microelectromech. Syst. 10 (2001) 41.
[26] L.V. Protsailo, W.R. Fawcett, Electrochim. Acta 45 (2000) 3497.
[27] P. Diao, D.L. Jiang, X.L. Cui, D.P. Gu, R.T. Tong, B. Zhong, J. Electroanal. Chem. 464 (1999) 61.
[28] H.O. Finklea, S. Avery, M. Lynch, T. Furtsch, Langmuir 3 (1987) 409.

[29] C. Boulas, J.V. Davidovits, F. Rondelez, D. Vuillaume, Phys. Rev. Lett. 76 (1996) 4797.
[30] V. Bertagna, R. Erre, F. Rouelle, M. Chemla, J. Solid State Electrochem. 4 (1999) 42.
[31] V. Bertagna, C. Plougonven, F. Rouelle, M. Chemla, J. Electroanal. Chem. 422 (1997) 115.
[32] A.M. Almanza-Workman, S. Raghavan, P. Deymier, D.J. Monk, R. Roop, J. Electrochem. Soc. 149 (2002) H6.
[33] A.M. Almanza-Workman, S. Raghavan, P. Deymier, D.J. Monk, R. Roop, Proceedings of the 198th Electrochemical Society Meeting 2000-19 (2000) 235.
[34] A.M. Almanza-Workman, S. Raghavan, P. Deymier, D.J. Monk, R. Roop, Diffus. Defect Data, Pt. B, Oostende, Belgium, Proceedings of the 5th International Symposium on Ultra Clean Processing of Silicon Surfaces 2000 76/77 (2001) 23.
[35] F.J. Kahn, Appl. Phys. Lett. 22 (1973) 386.
[36] A.Y. Fadeev, T.J. McCarthy, Langmuir 16 (2000) 7268.
[37] J.N. Israelachvili, M.L. Gee, Langmuir 5 (1989) 288.
[38] X. Cheng, G. Li, E.A. Kneer, B. Vermeire, H.G. Parks, S. Raghavan, J.S. Jeon, J. Electrochem. Soc. 145 (1998) 352.
[39] J.N. Chazalviel, Electrochim. Acta 35 (1990) 1545.
[40] J.R. Scully, R.P. Frankenthal, K.J. Hanson, D.J. Siconolfi, J.D. Sinclair, J. Electrochem. Soc. 137 (1990) 1365.
[41] J.R. Macdonald, Impedance Spectroscopy: Emphasizing Solid Materials and Systems, Wiley, New York, 1987.
[42] G.K. Jennings, J.C. Munro, T.H. Yong, P.E. Laibinis, Langmuir 14 (1998) 6130.
[43] M. Saakes, P.J. van Duin, A.C.P. Ligtvoet, D. Schmal, J. Power Sources 47 (1994) 149.